A Machine Learning Pipeline for Emotion Recognition based on Brain Topographic Maps Derived from Electroencephalogram Signals*

Bruno Cascaes Alves[1], Marla Pereira Melo[1], Artur Melchiori Cerri[2], Larissa Astrogildo de Freitas[1], Diana Francisca Adamatti[3], Marilton Sanchotene de Aguiar[1]

[1]Postgraduate Program in Computing, Federal University of Pelotas, Pelotas, Brazil
[2]Undergraduate in Computer Science, Federal University of Pelotas, Pelotas, Brazil
[3]Postgraduate Program in Computing, Federal University of Rio Grande, Rio Grande, Brazil
{bcalves,mrpmelo,amcerri,larissa,marilton}@inf.ufpel.edu.br; dianaada@gmail.com

Abstract

Emotion recognition is an increasingly relevant field due to its direct implications for various sectors of society. The area aims to enhance the understanding of how emotions influence human behavior. Exploring brain activity analysis through electroencephalogram signals becomes possible when considering that emotions can manifest non-verbally. In this scenario, machine learning applications prove promising due to the complexity of recognizing emotions from electrical signal data from the brain. The case study focuses on DEAP, a recognized dataset constructed through experiments in electroencephalography, exposing subjects to musical and visual stimuli. The main objective of this work is to present a pipeline for the classification of emotions based on images of topographic maps generated from the EEGLAB tool and electroencephalogram signals. Additionally, the contributions of this work include the presentation of a structured dataset created through the mapping of temporal, spatial, and frequency data derived from topographic images and models for predicting dimensional emotions of arousal and valence based on the new dataset. Results demonstrate accuracies of 85.46% and 85.05% for the classification of low/high arousal and valence emotions, respectively.

Introduction

Emotions are complex conditions described by mental states resulting from stimuli (Mauss and Robinson 2009). These mental states guide behavior to enhance adaptability to changes in the environment. Given the significance of emotions in human life, emotion recognition encompasses various applications, including medicine, neuroscience, and psychology (Niedenthal and Ric 2017).

Regarding the perspective of emotions, two methods can be used to categorize them: discrete and dimensional. The discrete perspective defines emotions through states such as joy and sadness. However, the dimensional perspective describes emotions based on scales. Two relevant emotional dimensions are arousal and valence, which are related to the degrees of intensity and pleasure, respectively (Hamann 2012).

Emotions can manifest non-verbally through indicators such as brain activity (Polzin 2000). Therefore, sensors can capture physiological signals to obtain emotion recognition. In particular, electroencephalogram (EEG) is a non-invasive procedure that analyzes brain electrical activity captured through electrodes positioned on the scalp. Thus, EEG plays an essential role in neuroscience by enabling the investigation of the human brain in various conditions and mental states (Sanei and Chambers 2021).

EEG signals are complex, exhibiting non-stationary and highly non-linear time series properties in the spatial, temporal, and frequency domains (Del Pozo-Banos et al. 2014). The spatial domain signifies the brain cortex region, the temporal domain indicates the event moment, and the frequency domain reflects the power. These EEG characteristics, with the subjectivity of emotions, present various challenges to this area. In this scenario, Machine Learning (ML) models enable the representation of systems through computational tools capable of identifying patterns in data and utilizing them for predictions (Alpaydin 2014).

Researchers in the literature focus on directly processing the brain signals (Samavat et al. 2022) or processing images from topographic maps (Sharma, Pachori, and Sircar 2020) to construct their systems. Specifically, topographic maps in the context of electroencephalography provide a graphical representation of the spatial distribution of brain electrical potential variations. Colors denote the frequency power spectrum, with lower power regions in dark blue and higher power regions in dark red. This method improves the comprehension of the relationships between brain activities in diverse regions (Hooi, Nisar, and Voon 2015).

This work focuses on the DEAP dataset (Koelstra et al. 2012), widely recognized and utilized in emotion recognition (Garg, Verma, and Singh 2023). It includes EEG signals from experiments exposing subjects to music video stimuli, who then self-assess on emotional dimensions.

Regarding this context, the present study proposes a machine learning-based pipeline for emotion classification using a novel structured dataset. We constructed the dataset by mapping data from images of topographic maps derived from the EEGLAB tool (Delorme and Makeig 2004) and

*This study was financed in part by the Coordenação de Aperfeiçoamento de Pessoal de Nível Superior – Brasil (CAPES) – Finance Code 001
Copyright © 2024 by the authors.
This open access article is published under the Creative Commons Attribution-NonCommercial 4.0 International License.

EEG signals. Based on the new dataset, we also developed models for emotion predictions, considering low or high intensity in the emotional dimensions of arousal and valence.

Theoretical Background

This Section presents fundamental concepts about electroencephalogram signals. Brain activity occurs through synapses when a neuron and another cell communicate. In this process, an electrical signal propagates and releases neurotransmitters, which are chemical substances responsible for transmitting the signal between neurons, generating a sequence of electrical and chemical events. Based on these signals, the central nervous system enables the perception, interpretation, and response to the environment (Squire et al. 2008).

These electrical events can be observed and measured through EEG, a procedure capable of detecting and recording the signals generated by the brain cortex using electrodes positioned on the scalp (Boutros et al. 2011). EEG signal acquisition follows electrode placement standards such as the International 10-20 System (Herwig, Satrapi, and Schonfeldt-Lecuona 2003), which specifies that the distance between electrodes should be either 10% or 20%, ensuring that the proportion between electrodes is maintained regardless of the individual's head size or the number of electrodes in the EEG device. As discussed, EEG signals exhibit spatial, temporal, and frequency aspects.

The spatial aspect corresponds to the location of the electrodes on the scalp about the lobes of the brain cortex. Each lobe is responsible for specific functionalities, namely: the Frontal Lobe F, responsible for motor control, decision-making, reasoning, personality, and emotional control; the Occipital Lobe O, dedicated to visual processing; the Parietal Lobe P, responsible for processing sensory information, including touch, temperature, and pain; and finally, the Temporal Lobe T, related to hearing, language processing, and memory (Tortora and Derrickson 2018).

Figure 1 illustrates the electrode placement locations for EEG devices with 32 channels based on the International System 10-20. In this system, odd and even numbers indicate the left and right hemispheres, respectively, and the suffix Z indicates the midline. The prefixes F (frontal) and C (central) refer to the frontal and central regions of the head together with Fp (prefrontal), AF (anterior frontal), and FC (frontal-central). The prefixes P (parietal) and CP indicate the parietal region. Finally, T refers to the temporal region, and O and PO indicate the occipital region.

The temporal aspect represents the dynamics of the brain over time. Segmenting the data using time windows to facilitate the EEG analysis is possible. The dynamic aspects of the brain over time lead to the use of these windows to divide the EEG signal into smaller parts (Casciola et al. 2021). For example, a 60-second EEG signal can be segmented using 1-second time windows (epochs), thus generating 60 signals.

Finally, the frequency aspect represents the power amplitude, as indicated by the signal's magnitude of oscillations per second. Five frequency bands can categorize these oscillations: i) Delta, characterized by high amplitude, occurs during deep sleep; ii) Theta, typically found in children and mental states of drowsiness; iii) Alpha, characterized by a lack of concentration; iv) Beta, typically found in adults and mental states of attention; and v) Gamma, characterized by low amplitude, occurs in states of mental hyperactivity (Sanei and Chambers 2021).

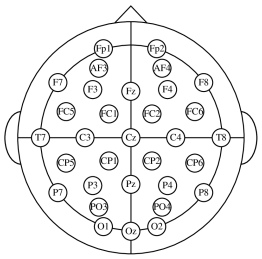

Figure 1: International 10-20 System of EEG with 32 electrodes. Source: (Abdelaal, Alsawy, and Hefny 2015)

Related Work

This Section aims to present the main related works, encompassing machine learning pipelines for emotion recognition using EEG signals from DEAP.

In (Qing et al. 2019), the authors proposed a pipeline for emotion identification by polarity, using a temporal window with 50% overlap and five frequency bands. It achieved a 63% accuracy independently of the subject with shallow ML algorithms, such as Decision Tree, K-Nearest Neighbors, and Random Forest. In (Asghar et al. 2019), the proposed system utilizes EEG signals mapped to spectrograms by Continuous Wavelet Transform (CWT) to recognize emotions in four quadrants: high valence with high arousal, high valence with low arousal, low valence with high arousal, and low valence with low arousal. The results indicated an average accuracy per subject of 77.4%, using Deep Learning (DL) for feature extraction and Support Vector Machine (SVM) for classification.

The system presented in (Sharma, Pachori, and Sircar 2020) can also classify emotions in four quadrants, using the EEG signals to create topographic maps with Third-order Cumulants for feature extraction across five frequency bands. This study achieved an average accuracy of 82% per subject with a model based on Long Short-Term Memory (LSTM). In (Demir et al. 2021), the authors developed binary models to classify high/low arousal and valence, generating spectrograms through CWT. Combining feature extraction by DL with the SVM classifier resulted in an accuracy of 91.07% for valence and 98.98% for arousal, considering the average across models developed for each subject.

Finally, the study of (Samavat et al. 2022) utilizes brain signals to construct a system for classifying emotions by polarity. It involves signal segmentation into two-second windows, feature extraction using Differential Entropy, and a Bi-LSTM block to incorporate temporal information into classification. The results demonstrate an accuracy of 72.38% using the Gamma band frequency.

Based on related work, the studies in the literature divide between directly processing the brain signal and processing mapped images of EEG signals. Furthermore, the excellent

results presented by the studies are centered on the classification of emotions for a given individual in models trained for this same individual. In the context of emotion recognition, this study proposes an approach based on images of brain topographic maps generated from EEG signals in EEGLAB. In contrast to previous works, our research introduces a structured dataset that maps brain activation levels by region from these images, providing a novel approach to EEG signal analysis. We leverage this constructed dataset to present predictive models trained with data from multiple individuals for arousal and valence, incorporating spatial, temporal, and frequency analyses.

Proposed Approach

This Section will present the proposed system for this study, detailing the emotion recognition pipeline and methodological decisions. We developed the pipeline using the OpenCV (Bradski and Kaehler 2008), Pandas (McKinney and others 2010), Scikit-Learn (Pedregosa et al. 2011) libraries in Python (Van Rossum and Drake 2009), and the EEGLAB tool (Delorme and Makeig 2004).

As illustrated in Figure 2, the beginning of the pipeline involves a set of EEG signals as input. A conversion process transforms these data into topographic images representing the brain. Subsequently, Digital Image Processing (DIP) techniques are applied to these images to segment the brain by electrodes (regions of interest). We map the activation levels in areas of the cortex through the colors of the pixels. Thus, we trained machine learning algorithms based on the data in a structured format. Finally, the pipeline allows for predictions, utilizing the best-performing ML models, to classify emotions from the perspective of low/high intensity in two dimensions: arousal and valence.

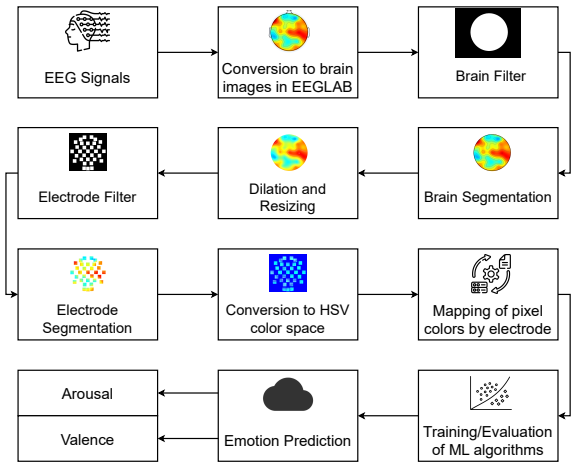

Figure 2: Overview of the proposed system.

In this scenario, the following methodological steps will be detailed: i) transformation of EEG signals into topographic maps and image processing; ii) construction of a structured dataset through mapping brain activation levels for each electrode using pixel colors in the images; and iii) development of predictive models for emotions using ML.

Topographic Maps Processing

The case study for this work is the DEAP dataset, as presented in Section 1. This dataset includes EEG signals collected from 32 participants using 32 electrodes. Each subject was exposed to 40 one-minute segments of music videos and provided emotional ratings for these stimuli in dimensions such as arousal and valence. These self-assessments range from one to nine on a continuous scale.

We used EEGLAB to explore and analyze the images derived from EEG signals. EEGLAB can generate images of brain topographic maps, illustrating the spatial distributions of brain electrical activities across time and frequency (Xu et al. 2020). Therefore, we generate topographic images in EEGLAB based on DEAP.

The resulting dataset contains 238,080 images capturing the brain activity of the 32 subjects who watched the 40 videos. Considering 62 one-second intervals, defined as windows, the script generated 62 images for each experiment. Thus, each image corresponds to a window data and covers one of three frequency bands represented by an intermediate sample: Alpha (10 Hz), Beta (22 Hz), or Gamma (42 Hz). We have not considered frequencies from the Delta and Theta bands because, as discussed in the background Section, they are common only in sleep. Additionally, we used only frequency samples due to the high processing time and the storage required to generate data.

Figure 3 shows three images generated during an experiment, each corresponding to a distinct brain frequency. The figure shows the activation level in brain regions through a color scale. Therefore, warm color pixels, such as dark red, represent regions with high brain activity. Intermediate color pixels, like yellow, represent regions of moderate brain intensity. Furthermore, cold color pixels, such as dark blue, represent regions with low brain activity.

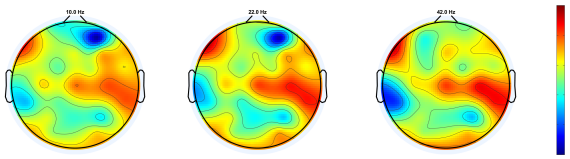

Figure 3: Example of topographic brain maps generated in EEGLAB for three frequencies.

The images generated contain information outside the region of brain activation of interest, such as lateral representations of the ears, nose, and sampling frequency. Using a filter called “Brain Filter” processes the images to eliminate these areas external to the circle representing the brain. We created this filter using the following DIP steps: conversion of an original image to grayscale, application of dilation to expand the object’s area around the pixels, and inverted binary thresholding, resulting in a filter that marks pixels from the region of interest as white and the rest as black.

Following this, we dilated the segmented images to remove lines within the brain and resized them from 875×656 to 250×250, keeping essential data. The subsequent process involves image segmentation based on electrode for-

mat using the "Electrode Filter" for analyzing brain regions. We constructed this filter from an image representing electrodes in the 10-20 International System, following the DIP steps: edge detection of each electrode using the Canny Edge (Canny 1986) algorithm; dilation to expand internal areas around the electrodes; transforming rounded shapes into quadrilaterals based on contour information, considering additional data from the area of the electrodes.

Finally, we convert the segmented brain electrode images from RGB to the HSV color space. After this, the pixels of the images are described through the hue, saturation, and value properties and no longer by the mixture of primary colors (red, green, and blue). Respectively, hue, saturation, and value are related to the color tone, purity, and brightness (Gonzales and Woods 2019). This conversion provides an alternative form to represent colored images closer to human perception of colors.

Structured Dataset

Based on the image segments described in the previous Section, it becomes possible to create a structured dataset that organizes the image data mapping according to the level of brain activation and the corresponding electrode areas.

Considering that the colors in the images generated in EEGLAB correspond to the level of brain activity, as shown in Figure 3, the pixel colors can establish a heuristic relationship with low, medium, and high levels of brain activity. Thus, to construct the structured dataset based on OpenCV scales, we map low brain activity segments with hue values from 90 to 150 (cold colors), medium activity with hue from 30 to 90 (intermediate colors), and high activity with hue values from 150 to 30 (warm colors). Saturation limits range from 80 to 255, and value limits range from 40 to 255.

Therefore, it is possible to determine the percentage of pixels associated with each electrode to different levels of brain activity. For example, assuming there are 100 pixels over an electrode and 5 of these pixels are cold colors, 25 are intermediate colors, and 70 are warm colors, we can interpret that, respectively, 5% of the electrode exhibits low levels of brain activity, 25% medium, and 70% high levels.

The mapping of brain activation levels by electrodes, combined with the tabular data detailed in DEAP, allows the construction of a structured and unified dataset. Thus, the entries of the structured dataset include subject and experiment identification, epoch and sampling frequency, and subjects' self-assessments related to two emotion scales: arousal and valence. Furthermore, the dataset contains 32 columns for each of the 32 EEG signal electrode channels in DEAP, where the entry in each of these columns consists of a tuple representing the percentage of brain activation at low, medium, and high levels in that order. In this way, the complete dataset consists of 38 columns and 238,080 records.

The constructed structured dataset provides an alternative format for EEG data analysis. This dataset allows specific experiments, distinguishing itself from raw and image formats. The drawbacks of raw and image data include interpretability issues and the need for extensive storage and processing capacity, especially in the last format.

Emotion Predictor Models

We divided the EEG signals into segments corresponding to the mapping of each electrode arranged in a structured dataset, as discussed in the previous Section. Each electrode can contribute to emotion recognition, as it contains data about the percentage levels of activation categorized as low, medium, and high. Therefore, it is possible to estimate emotion classes based on the intensity of brain activation.

To investigate the relevance of brain regions in emotion prediction, we generated 11 combinations based on electrode mapping. Table 1 details these configurations used in the experiments, indicating the number of attributes for each dataset. For example, the Temporal region consists of electrodes with the prefix `T`, totaling two attributes.

Table 1: Configuration of the dataset regarding its attributes.

Dataset	Attributes	Total
All	AF3, AF4, CZ, C3, C4, CP1, CP2, CP5, CP6 FZ, F3, F4, F7, F8, FC1, FC2, FC5, FC6, Fp1, Fp2 PZ, P3, P4, P7, P8, PO3, PO4, OZ, O1, O2, T7, T8	32
AF	AF3, AF4	2
C	CZ, C3, C4	3
CP	CP1, CP2, CP5, CP6	4
F	FZ, F3, F4, F7, F8	5
FC	FC1, FC2, FC5, FC6	4
Fp	Fp1, Fp2	2
P	PZ, P3, P4, P7, P8	5
PO	PO3, PO4	2
O	OZ, O1, O2	3
T	T7, T8	2

The preprocessing steps for the tabular data for the arousal and valence targets are specified below. Initially, we transformed the values from a continuous format, ranging from 1 to 9, to a binary format, allowing the models to make predictions from a low (0) or high (1) perspective. The ideal value to split the dimensions would be 5, the mean of the rating scale. However, it was necessary to balance the data. This operation involved setting specific thresholds to use the highest number of records, with thresholds of 5.25 for arousal and 5.04 for valence. Additionally, random removal of rows was applied to address valence imbalances, removing 124 records. Due to missing data, we excluded experiments 12 and 24 for subject 11 from our models.

In addition to assessing the frequency variation at 10, 22, and 42 Hz and spatial aspects, it is possible to explore temporal aspects through EEG signals. For this, temporal windows of 1, 4, 10, and 20 seconds were considered, with 50% overlap for windows longer than one second. For example, considering an 8-second signal with a 4-second window and 50% overlap, we would have three combined segments: 0 to 4, 2 to 6, and 4 to 8. The averaging of percentage levels yields the combinations for each electrode's segment.

With the data properly adjusted, the next step involved stratifying the division into training and testing sets. Thus, we allocate 80% of the data to training classification algorithms and 20% to testing the performance of the constructed models. Table 2 shows the number of records, by frequency, for training and testing for each emotional dimension and each type of configuration related to temporal windows.

Considering the constructed dataset and the spatial, temporal, and frequency configurations, three classification al-

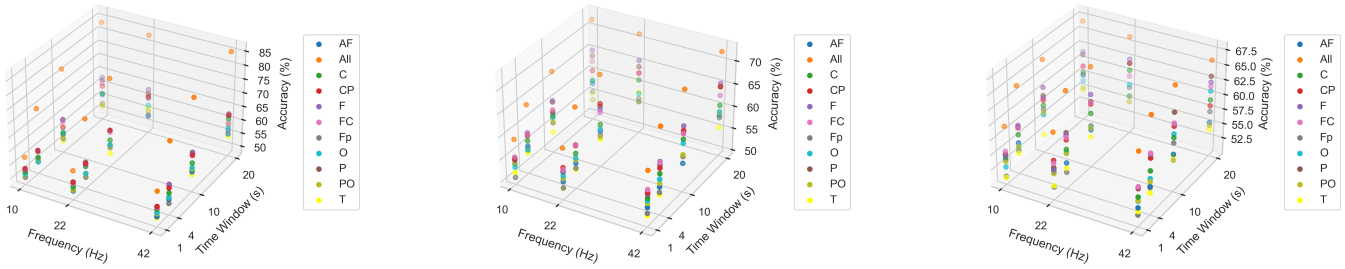

Figure 4: Arousal accuracies. From left to right, the charts show the results of the K-NN, RF, and SVM algorithms.

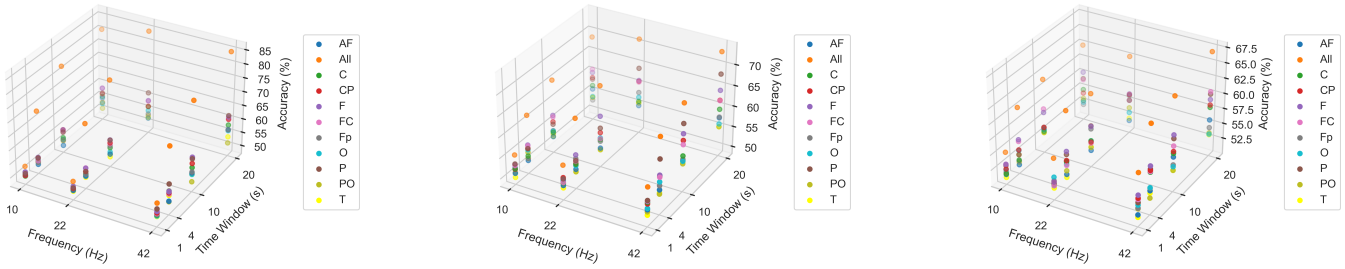

Figure 5: Valence accuracies. From left to right, the charts show the results of the K-NN, RF, and SVM algorithms.

Table 2: Training and testing dataset configurations.

Target	Temporal window configuration							
	1 second		4 seconds		10 seconds		20 seconds	
	Train	Test	Train	Test	Train	Test	Train	Test
Arousal	63,388	15,848	30,672	7,668	12,268	3,068	6,134	1,534
Valence	63,290	15,822	30,624	7,656	12,250	3,062	6,124	1,532

Table 3: Input hyperparameters.

Algorithm	Hyperparameters
K-NN	{'n_neighbors': [**1**, 3, 5, 7, 9]}
RF	{'n_estimators': [100, **200**], 'max_depth': [10, **None**]}
SVM	{'C': [0.1, 1, **2**]}

gorithms were trained and evaluated: i) K-Nearest Neighbors (K-NN), this algorithm predicts based on the majority of training examples closest/similar in a multidimensional space (Sanei and Chambers 2021); ii) Random Forest (RF), this algorithm calculates the majority vote of predictions generated by a group of decision trees (Alpaydin 2014); and iii) Support Vector Machine (SVM), this algorithm seeks the maximum margin that separates the hyperplane to gather the most significant number of data in a area (Geron 2019).

The hyperparameters of the algorithms were determined using the Grid Search (LaValle, Branicky, and Lindemann 2004) technique to identify the best combination of inputs for each model. Table 3 describes the input hyperparameters considering the Scikit-Learn (Pedregosa et al. 2011) library for K-NN, RF, and Radial Basis Function kernel SVM. The previously separated training data were applied using cross-validation in five distinct groups, with five iterations, to assess the model's generalization capability. Thus, each iteration refers to the set with validation data and the rest to the training data. The criterion chosen to determine the best performance among different hyperparameter configurations was the F1-Score, given its suitability for creating rankings. In general, we developed the best-performing models based on the hyperparameters in bold in Table 3.

In this context, we generate at least 396 models per target, considering three frequencies (10, 22, and 42 Hz), 11 combinations of brain regions (Table 1), four temporal window configurations (Table 2), and three ML algorithms (Table 3).

Results and Discussions

This Section will present the results of this study. Thus, we will discuss the results of the models developed for emotion prediction, considering the dimensions of arousal and valence. For this study, we utilized four metrics for evaluating classifiers: accuracy, precision, recall, and F1-Score. Higher values indicate superior results, as reflected in the metrics.

Figures 4 and 5 respectively describe accuracy results for the models constructed targeting arousal and valence. There are three charts for each of these figures, representing the central classifiers of this study. These charts consider the essential features of EEG signals, including spatial, temporal, and frequency domains. When analyzing these charts, it is possible to observe the distribution of points along the axes, enabling the identification of patterns in the data.

The models created using the `All` dataset show promising performances in configuration scenarios compared to datasets composed of attributes related to specific electrode regions, both for arousal and valence. Thus, the results emphasize the significance of this composition, where the models rely on data from all 32 EEG electrodes.

Although the arousal and valence results exhibit similarities in accuracy values by configuration, there are particularities. For instance, the independent brain region that showed

Table 4: Results of classification models for the best and worst cases.

Emotion	Temporal Window (s)	Frequency (Hz)	Brain Region	Precision (%)		Recall (%)		F1-Score (%)		Accuracy (%)
				Class 0	Class 1	Class 0	Class 1	Class 0	Class 1	
Best Case (K-NN)										
Arousal	20	42	All	85.51	85.42	85.4	85.53	85.45	85.47	85.46
Valence	20	42	All	85.01	85.1	85.12	84.99	85.06	85.04	85.05
Worst Case (K-NN)										
Arousal	1	10	Fp	49.82	49.84	47.73	51.93	48.75	50.86	49.83
Valence	10	10	AF	49.54	49.54	49.31	49.77	49.43	49.66	49.54

more promising results in a specific format differs for both dimensions. In this scenario, the model based on attributes from the frontal region F at 22 Hz demonstrated an accuracy of 65.71% for arousal. In comparison, the model with attributes from the parietal region P at 42 Hz achieved an accuracy of 64.56% for valence. In both cases, we constructed these models using RF and a longer temporal window.

In general terms, the results of this case study indicate that F and P datasets, along with central adjacent configurations FC and CP, may be relevant for exploratory studies of patterns in specific brain regions. As discussed in the Background Section, the frontal region is a brain area related to emotion control. However, dataset configurations with fewer attributes, such as the temporal T, often showed less favorable results.

We constructed models for three frequency samples in the Alpha, Beta, and Gamma bands. Based on the results, models with Beta and Gamma frequency bands performed better than the Alpha band, especially with temporal windows exceeding 1 second. Notably, frequencies in the Alpha band are associated with a state of relaxation. When analyzing the variation in temporal windows, we observe a constant performance for all algorithms with a 1-second window, with SVM standing out positively at 42 Hz. However, we note a significant improvement when using 4-second temporal windows or more. The K-NN algorithm stands out positively for temporal windows exceeding 1 second with overlap, especially considering data from all electrodes.

To support the results in the charts, Table 4 summarizes the results for the emotion models created in this study for the best and worst cases. According to this table, the best results for arousal and valence pertain to models constructed using longer temporal windows, a frequency of 42 Hz, and the use of data from all EEG signal electrodes. Upon examining the metrics, it is noticeable that the models do not explicitly prefer predicting one class significantly more than the other. Furthermore, the models based on shorter temporal windows, 10 Hz, for brain regions related to datasets with fewer attributes generated the worst results. K-NN was the algorithm responsible for constructing the best and worst-case models. Thus, despite its simplicity, this algorithm can apply to complex problems, with the observation that it is directly affected by the attributes used.

Generally, studies in the literature base them on constructing specific models for each individual, which can lead to superior performance. However, this work created models trained with data from multiple subjects using a novel data format. Thus, the results were promising, considering the complexity of the field, either due to the complex nature of EEG signals or the subjectivity of emotions.

Conclusion and Future Works

This work proposes an ML pipeline for emotion recognition based on brain topographic maps derived from EEG signals, using the DEAP dataset as a case study. With a focus on this theme, the main objectives were to construct a structured dataset by mapping brain regions and their respective activation intensities in the topographic maps generated using the EEGLAB tool. Additionally, the study involved analyzing and developing predictive models for emotions.

The constructed dataset provides an alternative approach for analyzing data in EEG-based emotion recognition tasks. We constructed predictive models using machine learning techniques, utilizing approximately 238 thousand records from the constructed structured dataset in the experiments. Three classification algorithms, K-NN, RF, and SVM, were trained. We developed models with frequency, spatial, and temporal variations in each algorithm experiment.

About the results, using data from all electrodes positively contributed to the performance of predictive models. However, when analyzing specific brain regions, the frontal area stands out positively. Furthermore, models created with data in the Beta and Gamma frequencies yielded more efficient results, especially at 42 Hz. The use of temporal windows proved effective, with consistent results even with 4-second windows, considering the complexity of the data. Respectively, the K-NN and SVM algorithms demonstrated more satisfactory responses in the emotion prediction task, especially when using temporal windows with and without overlap. Thus, the results show models with an accuracy of 85.46% and 85.05% for the classification of low/high arousal and valence emotions, respectively, with a 20-second window, a frequency of 42 Hz, K-NN, and all electrodes.

This research represents a relevant study topic in the context of emotion recognition through EEG signals, transformed into topographic maps and mapped into a structured dataset. The structured approach for analysis and model construction allows for an alternative format to analyze the behavior and functioning of the human brain through emotion, making it attractive for the field of neuroscience.

For future work, the intention is to explore and develop new models for emotion recognition, considering different frequency and temporal samples. Additionally, there are plans to conduct additional experiments with the structured dataset, exploring new combinations of brain regions. Another line of research will involve conducting experiments using the topographic map dataset with segmented brain regions using deep learning algorithms.

References

Abdelaal, M.; Alsawy, A.; and Hefny, H. 2015. On emotion recognition using eeg. In *The 50th Annual Conference on Statistics, Computer Sciences and Operations Research*, 35–49.

Alpaydin, E. 2014. *Introduction to Machine Learning*. Cambridge, MA, USA: MIT Press, 3 edition.

Asghar, M. A.; Khan, M. J.; Fawad; Amin, Y.; Rizwan, M.; Rahman, M.; Badnava, S.; and Mirjavadi, S. S. 2019. Eeg-based multi-modal emotion recognition using bag of deep features: An optimal feature selection approach. *Sensors* 19(23).

Boutros, N.; Galderisi, S.; Pogarell, O.; and Riggio, S. 2011. *Standard Electroencephalography in Clinical Psychiatry*. New Jersey, USA: Wiley, 1st edition.

Bradski, G., and Kaehler, A. 2008. *Learning OpenCV: Computer vision with the OpenCV library*. Sebastopol, CA, USA: O'Reilly Media, Inc.

Canny, J. 1986. A computational approach to edge detection. *IEEE Transactions on pattern analysis and machine intelligence* PAMI-8(6):679–698.

Casciola, A.; Carlucci, S.; Kent, B.; Punch, A.; Muszynski, M.; Zhou, D.; Kazemi, A.; Mirian, M.; Valerio, J.; McKeown, M.; and Nygaard, H. 2021. A deep learning strategy for automatic sleep staging based on two-channel eeg headband data. *Sensors* 21:3316.

Del Pozo-Banos, M.; Alonso, J. B.; Ticay-Rivas, J. R.; and Travieso, C. M. 2014. Electroencephalogram subject identification: A review. *Expert Systems with Applications* 41(15):6537–6554.

Delorme, A., and Makeig, S. 2004. Eeglab: an open source toolbox for analysis of single-trial eeg dynamics including independent component analysis. *Journal of Neuroscience Methods* 134(1):9–21.

Demir, F.; Sobahi, N.; Siuly, S.; and Sengur, A. 2021. Exploring deep learning features for automatic classification of human emotion using eeg rhythms. *IEEE Sensors Journal* 21(13):14923–14930.

Garg, D.; Verma, G.; and Singh, A. 2023. A review of deep learning based methods for affect analysis using physiological signals. *Multimedia Tools and Applications* 82:46.

Geron, A. 2019. *Hands-On Machine Learning with Scikit-Learn, Keras, and TensorFlow: Concepts, Tools, and Techniques to Build Intelligent Systems*. Sebastopol, CA, USA: O'Reilly Media, Inc., 2nd edition.

Gonzales, R., and Woods, R. 2019. *Digital Image Processing*. New York, USA: Pearson, 4 edition.

Hamann, S. 2012. Mapping discrete and dimensional emotions onto the brain: controversies and consensus. *Trends in Cognitive Sciences* 16(9):458–466.

Herwig, U.; Satrapi, P.; and Schonfeldt-Lecuona, C. 2003. Using the international 10-20 eeg system for positioning of transcranial magnetic stimulation. *Brain topography* 16:95–99.

Hooi, L. S.; Nisar, H.; and Voon, Y. V. 2015. Tracking of eeg activity using topographic maps. In *2015 IEEE International Conference on Signal and Image Processing Applications (ICSIPA)*, 287–291.

Koelstra, S.; Muhl, C.; Soleymani, M.; Lee, J.-S.; Yazdani, A.; Ebrahimi, T.; Pun, T.; Nijholt, A.; and Patras, I. 2012. Deap: A database for emotion analysis using physiological signals. *IEEE Transactions on Affective Computing* 3(1):18–31.

LaValle, S. M.; Branicky, M. S.; and Lindemann, S. R. 2004. On the relationship between classical grid search and probabilistic roadmaps. *The International Journal of Robotics Research* 23(7-8):673–692.

Mauss, I. B., and Robinson, M. D. 2009. Measures of emotion: A review. *Cognition and Emotion* 23(2):209–237. PMID: 19809584.

McKinney, W., et al. 2010. Data structures for statistical computing in python. In *Proceedings of the 9th Python in Science Conference*, volume 445, 51–56. USA: SciPy.

Niedenthal, P. M., and Ric, F. 2017. *Psychology of emotion*. New York, USA: Psychology Press.

Pedregosa, F.; Varoquaux, G.; Gramfort, A.; Michel, V.; Thirion, B.; Grisel, O.; Blondel, M.; Prettenhofer, P.; Weiss, R.; Dubourg, V.; et al. 2011. Scikit-learn: Machine learning in python. *Journal of machine learning research* 12(Oct):2825–2830.

Polzin, T. 2000. Verbal and non-verbal cues in the communication of emotions. In *2000 IEEE International Conference on Acoustics, Speech, and Signal Processing.*, volume 4, 2429–2432. USA: IEEE.

Qing, C.; Qiao, R.; Xu, X.; and Cheng, Y. 2019. Interpretable emotion recognition using eeg signals. *IEEE Access* 7:94160–94170.

Samavat, A.; Khalili, E.; Ayati, B.; and Ayati, M. 2022. Deep learning model with adaptive regularization for eeg-based emotion recognition using temporal and frequency features. *IEEE Access* 10:24520–24527.

Sanei, S., and Chambers, J. 2021. *EEG Signal Processing and Machine Learning*. New Jersey, USA: Wiley, 2nd edition.

Sharma, R.; Pachori, R. B.; and Sircar, P. 2020. Automated emotion recognition based on higher order statistics and deep learning algorithm. *Biomedical Signal Processing and Control* 58:101867.

Squire, L.; Berg, D.; Bloom, F. E.; Du Lac, S.; Ghosh, A.; and Spitzer, N. C. 2008. *Fundamental Neuroscience*. Massachusetts, USA: Academic Press, 3rd edition.

Tortora, G., and Derrickson, B. 2018. *Introduction to the Human Body*. New Jersey, USA: Wiley, 11th edition.

Van Rossum, G., and Drake, F. L. 2009. *Python 3 Reference Manual*. Scotts Valley, CA: CreateSpace.

Xu, M.; Yao, J.; Zhang, Z.; Li, R.; Yang, B.; Li, C.; Li, J.; and Zhang, J. 2020. Learning eeg topographical representation for classification via convolutional neural network. *Pattern Recognition* 105:107390.